energies

MDPI

Article

Optimization of Energy Recovery Processes from Sunflower Stalks Using Expired Non-Steroidal Anti-Inflammatory Drugs (NSAIDs)

Valentina Zubkova [1], Andrzej Strojwas [1,*] and Stanislaw Baran [2]

[1] Institute of Chemistry, Faculty of Sciences and Natural Sciences, Jan Kochanowski University in Kielce, Uniwersytecka Str. 7, 25-406 Kielce, Poland; walentyna.zubkowa@ujk.edu.pl
[2] M. Smoluchowski Institute of Physics, Faculty of Physics, Astronomy and Applied Computer Science, Jagiellonian University, Lojasiewicza Str. 11, 30-348 Krakow, Poland; stanislaw.baran@uj.edu.pl
* Correspondence: andrzej.strojwas@ujk.edu.pl

Abstract: The influence of the addition of expired paracetamol, naproxen, ibuprofen, and their blend on the course of pyrolysis of sunflower stalks was studied using the gravimetric technique as well as the techniques of IR and UV, XRD, and SEM and EDX spectroscopies. It was ascertained that ibuprofen has the highest effect in reduction of hydrocarbons in the composition of volatile pyrolysis products, which lowers the contribution of bands: saturated and unsaturated hydrocarbons by about 2.36 times; compounds with carbonyl groups by almost by three times; and the contribution of alcohols, phenols, and esters by 2.5 times in the FT-IR spectra. The reasons for a greater effectiveness of ibuprofen in reducing hydrocarbons in volatiles can be its lower temperature of decomposition and distinct composition of formed volatile pyrolysis products. Up to the temperature of 450 °C, paracetamol inhibits the migration of AAEMs from the pyrolyzed sample, the blend of pharmaceuticals accelerates the migration of all AAEMs except inorganics with Mg atoms. In the sediment of char of ibuprofen additive, there is a higher amount of Ca, Mg, and Cl atoms than in other chars, which can explain a greater influence of ibuprofen on the reduction of hydrocarbons in the composition of volatiles.

Keywords: energy recovery; circular bioeconomy; NSAIDs disposal

Academic Editors: Carmen Otilia Rusănescu and Nicoleta Ungureanu

Received: 19 February 2025
Revised: 10 March 2025
Accepted: 13 March 2025
Published: 18 March 2025

Citation: Zubkova, V.; Strojwas, A.; Baran, S. Optimization of Energy Recovery Processes from Sunflower Stalks Using Expired Non-Steroidal Anti-Inflammatory Drugs (NSAIDs). *Energies* **2025**, *18*, 1509. https://doi.org/10.3390/en18061509

1. Introduction

The withdrawal of fossil fuels from energy production and the adaptation to the circular bioeconomy require a more rational approach to the thermal processing of biomass, including agricultural biomass waste. From the viewpoint of carbon neutrality, biomass is perceived as a good source of energy. However, the presence of polycyclic aromatic hydrocarbons, polar compounds, and compounds containing carbonyl groups in volatile products of biomass decomposition can lead to their aggregation and formation of particulate matters (PM) [1,2] that negatively affect human health and the natural environment.

In order to dispose of compounds polluting the environment, the optimization of biomass energy processing should be achieved in two ways:

(a) to develop the construction of appropriate technical devices and apparatus in the form of various purifying filters, adsorbers, and absorbers, removing harmful substances from volatile products of biomass pyrolysis;
(b) to introduce the so-called auxiliary raw materials into the composition of processed biomass, the use of which leads to a reduction of harmful compounds in the composition of pyrolysis products in the energy recovery process.

The first way requires high investment costs and costs connected with the use of chemical reagents or regeneration of adsorbents and absorbers. The second way seems to be much simpler and cheaper provided that wastes are taken as auxiliary raw materials.

Sunflower stalks are attributed to the waste biomass emerging during vegetable oil production. Sunflower oil is the second most popular vegetable oil in Poland. The world production of sunflower oil reaches almost 21 million tons and Poland's participation in its imports was 13.3%. The wastes from oil production are generated in many farms and cause certain problems with regard to their energy utilization for local farmers. So far, no effective and simple methods for energy recovery from these wastes on small farms have been proposed due to the lack of information on threats that may arise during energy processing.

Organic wastes include expired pharmaceuticals that are generated in households and require high disposal costs. The non-steroidal anti-inflammatory drugs (NSAIDs) available in pharmacies without prescription constitute the largest group of expired waste. Mgharbel et al. [3] suggest that the pyrolysis of pharmaceutical wastes can be an ecologically sufficient and an economically sustainable treatment of pharmaceutical wastes in the context of circular economy. The expired NSAIDs were added to hard bituminous coals in order to improve the plastic properties of a high volatile bituminous coal [4] and to decrease the coking pressure of dangerous coals [5]. It was stated recently that expired pharmaceuticals can be disposed during their co-pyrolysis with specific types of biomass, reducing the amount of hydrocarbons in the composition of volatile products [6]. It was ascertained in this publication that paracetamol and naproxen additives reduce the presence of harmful compounds during their co-pyrolysis with pea husks, do not change the composition of volatiles from their co-pyrolysis with corn cobs, and increase the presence of undesirable substances during co-pyrolysis with sunflower insolence.

Similar to other agricultural biomass species, sunflower stalks are classified as lignocellulosic biomass, the main components of which (hemicellulose, cellulose, and lignin) are decomposed during pyrolysis in certain temperature ranges [7]. Aldehydes, ketones, phenols, alcohols, furan, and pyran compounds, along with other reactive chemical compounds, are present in the composition of products of their thermal decomposition [8–10]. The explanation of the mechanism of thermochemical changes taking place in samples of lignocellulose biomass is a complex task that faces many difficulties. There are some interactions between the components of biomass and the products of their decomposition during pyrolysis that affect both the yield of pyrolysis products [11–13] and their composition [14–16]. Moreover, during pyrolysis interactions occur between the volatile products of pyrolysis and the formed char that regulate the course of secondary reactions between compounds present in the gas phase [17–19]. Apart from biogenic elements, biomass also contains inherent inorganic species that occur in the form of metalloporphyrins, which are organic minerals such as Ca-Mg-K-Na oxalates, organic calcium compounds, soluble salts, insoluble minerals, etc. [20–22]. It has been established that inorganics can influence the thermal behaviour of biomass, and change the yield of pyrolysis products [20,23] and the composition of volatile products [21,24–27]. During the process of pyrolysis, inorganics can migrate in a pyrolyzed sample and escape from biomass together with volatile products [28,29]. The migration process of inorganics can lead to changes in their concentration in the studied samples, thus affecting the interaction between biomass components and the volatile–char interactions.

In light of the currently prevailing principles of circular economy, it made sense to investigate the influence of expired NSAIDs such as paracetamol, naproxen, and ibuprofen on the changes in composition of volatile products of pyrolysis of sunflower stalks and to evaluate the impact of each additive. Taking into account the possibility of collecting

expired pharmaceuticals and segregating them into types, it was essential to study the influence of a 1:1:1 blend of paracetamol, naproxen, and ibuprofen on the changes in composition of volatiles and present the characteristics of the obtained pyrolysis products

2. Materials and Methods

2.1. Materials

The research objects (sunflower stalks) were washed in distilled water and dried first at room temperature and then in a vacuum drier (VDL23 manufactured by Binder GmbH, Tuttlingen, Germany). Sunflower stalks (SS) were blended with the crushed tablets of expired NSAIDs, such as naproxen (NP), paracetamol (PR), ibuprofen (IB), and their ternary blend (BL). According to the IUPAC nomenclature, paracetamol (called N-(4-hydroxyphenyl) acetamide was the pharmacologically active substance in APAP tablets, naproxen (called 2-(6-methoxynaphthalen-2-yl) propanoic acid) in Apo-Napro tablets, and Ibuprofen (called (RS)-2-(4-(2-methylpropyl)phenyl)propanoic acid) in IBUPROM tablets. Before testing, tablet coatings containing excipients were removed.

An Elementar Vario Micro Cube CHNS Analyzer (Elementar Analysensysteme GmbH, Langenselbold, Germany) was used for the ultimate analysis of a single SS sample, and the content of inorganic elements was determined with a Thermo Scientific Niton Goldd+ analyzer (Thermo Fisher Scientific Inc., Waltham, MA, USA). Table 1 presents the characteristics of the SS sample.

Table 1. The characteristics of SS sample.

Ultimate analysis [%]	
C^d	44.60 ± 0.02
H^d	6.05 ± 0.01
N^d	0
S^d	0
A^d	4.91 ± 0.08
O^{adiff}	43.44 ± 0.04
Content of inorganic elements [mg·kg^{-1}]	
Si	4728 ± 277
P	280 ± 113
S	1442 ± 86
Cl	4931 ± 62
K	7476 ± 115
Ca	26,344 ± 421
Zn	37 ± 5
Higher Heating Value [MJ·kg^{-1}]	
HHV^b	17.99 ± 0.12

[(a)] calculated by difference, O^{diff} [%] = 100 − C − H − N − S − Ash; [(b)] calculated by HHV [MJ·kg^{-1}] = 0.3491·C^d + 1.1783·H^d + 0.1005·S^d − 0.0151·N^d − 0.1034·O^{diff} − 0.0211·A^d; [(d)] dry basis.

The confidence interval in the determination of inorganic content was checked by comparison with the reference materials: NIST-1575a (Pine Needles), NIST-1573a (Tomato leaves), and IC-INCT-PVLT-6 (Tobacco leaves). As shown in Table 1, the excessive content of O element in the SS sample can result in an increased content of oxygen-containing compounds in the products of its pyrolysis and combustion. The values of the HHV parameter of the SS sample are similar to those of other biomass types studied in works by other authors [30,31], which confirms the possibility of using SS wastes in energy recovery.

The SS sample and the tablets of expired pharmaceuticals were ground to grains of <0.2 mm in size. The blends with SS were prepared from the ground material with the

additions of 2 wt.% of NP, PR, IB, and BL. Weighing was performed on a Precisa 92SM-202A analytical balance (Precisa Instruments AG, Dietikon, Switzerland) with an accuracy of four decimal places. The prepared blends were densified into tablets with the following density: with NP—1.035 ± 0.035 g·cm^{-3}, with PR—1.027 ± 0.019 g·cm^{-3}, with IB—1.028 ± 0.023 g·cm^{-3}, and with BL—1.031 ± 0.025 g·cm^{-3}. The density of tablets of the SS sample without additives was 1.011 ± 0.014 g·cm^{-3}.

2.2. Methods

2.2.1. Pyrolysis of Studied Samples

The densified samples were heated to a temperature of 780 °C in a Q50 thermobalance (TA Instruments Inc., New Castle, DE, USA) under a high-purity nitrogen atmosphere with the heating rate of 10 °C·min^{-1}. The carrier gas flow rate through the thermobalance was 10 mL·min^{-1}, and through the transfer line, 90 mL·min^{-1}. The TGA curves of the weight loss of samples were recorded along with the DTG curves of the weight loss rate. The obtained DTG curves were deconvoluted with an OMNIC9.2.86 software to determine the contribution of basic components of biomass in the formation of these curves according to the procedure described in works [32,33]. During the deconvolution of DTG curves, the temperature ranges of decomposition of hemicellulose, cellulose, and lignin [7] were taken into account.

Figure S1 presents the examples of DTG curve fittings. The fitting was performed automatically after assigning the Gaussian/Lorentzian function. The surface areas of sub-peaks corresponding to the weight loss rate of biomass components were calculated by software. The contribution of individual components was calculated assuming the surface of DTG peak as 100%. The changes in the surface of the sub-peak of the studied component indicate changes in its thermal stability and its contribution to the formation of the DTG curve under the influence of the additive. The volatile products of pyrolysis were transported via Interface (Thermo Fisher Scientific Inc.) to a Nicolet iS10 spectrometer (Thermo Fisher Scientific Inc.), by which their FT-IR spectra were registered.

The FT-IR spectra were elaborated by an OMNIC9.2.86 software in order to remove the non-specific background and to measure the surface of bands. Moreover, the FT-IR spectra of volatile products were normalized with regard to the height of CO_2 band. The ratios of surfaces of the bands assigned to saturated and unsaturated hydrocarbons (A_{CH}, the range of wavenumbers of 3250–2500 cm^{-1}), compounds with carbonyl groups (A_{CO}, the range of wavenumbers of 1900–1600 cm^{-1}), alcohols, phenols, and esters (A_{APE}, the range of wavenumbers of 1320–900 cm^{-1}) to the surface of CO_2 band (A_{CO2}) were calculated. The obtained ratios were taken into account during the analysis of the influence of the used additives on the changes in contribution of hydrocarbons in the composition of volatile products of studied samples. Additionally, the expired pharmaceuticals and their blend (1:1:1) were pyrolyzed separately in a thermobalance under the same conditions as the biomass samples. The TGA and DTG curves along with the FT-IR spectra of volatile products of pyrolysis of the additives (PR, NP, IB, and BL) were recorded.

In parallel, all studied samples were put in quartz cuvettes, then placed in a Czylok (Company PRC 70x708/110 M, Jastrzębie-Zdrój, Poland) tube furnace and pyrolyzed under a 99.999% nitrogen atmosphere with an average heating rate of 10 °C·min^{-1} to a temperature of 450 °C. The carrier gas flow rate was 330 mL·min^{-1}. The isothermal hold was 30 before cooling in nitrogen. The formed volatiles were passed through a methanol layer cooled by ice-water to obtain a material condensed in methanol.

2.2.2. Spectroscopic Investigations

After removal of methanol, the condensates were kept under a vacuum until their weight was constant and then studied in a Nicolet iS10 spectrometer equipped with a

Smart MIRacle module and ZnSe monocrystal. The ATR spectra were recorded in the wavenumber range of 4000–600 cm^{-1}. OMNIC9.2.86 software was applied to remove the non-specific background, to include the local optical minima, and to normalize spectra automatically to make their visual comparison easier. The height of the band near the wavenumber of 1600 cm^{-1} was taken as reference because it corresponds to the bonds of C=C type.

Next, the condensates weighing 0.0001 g were poured into a laboratory glass beaker and dissolved in 50 mL of acetonitrile. The dissolution was ultrasonically assisted. The recording of spectra was conducted in a double-beam Jasco V-630 spectrophotometer in the wavelength range of 190–350 nm. The UV spectra were normalized at the wavelength of 190 nm by a Jasco Spectra Manager II software version 2.08.04.

2.2.3. Investigations of Chars

The XRD, SEM, and EDX techniques were used to analyze the obtained chars. The samples were first heated in a tube furnace to a temperature of 450 °C and then studied at room temperature with an X'Pert Pro X-ray diffractometer (PANalytical Company, Malvern, UK). The diffractometer modes were as follows: U = 40 kV, I = 45 mA, range of 2θ = 10–55 deg., with a step of 0.033 deg. Before analysis, all samples were crushed in an agate mortar. Additionally, 10% NaF used as an internal standard was added to the samples prepared this way and then mixed well. The samples were weighed by a Precisa analytical balance with the accuracy of four decimal places. The normalization of diffractograms was conducted with respect to the height of (002) the reflex from NaF. The calculations of ratios of the integral intensity of common reflex of γ-fraction and (002) chars to the integral intensity of (002) reflex from NaF were carried out along with those of inorganics.

The chars heated to a temperature of 750 °C in a Q50 thermobalance were separated into surface, subsurface, and inner layers, then pasted onto the adhesive tape of the sampler and placed in a Quanta 3D FEG scanning electron microscope (SEM). The EDX microanalysis was carried out to obtain information about the elemental composition of the material of separated layers of chars from all samples. The accelerating voltage was 20 keV.

3. Results and Discussion

3.1. Changes in Composition of Volatile Products of Pyrolysis

Figure 1 presents the FT-IR spectra of volatile products from the SS sample and its blends with pharmaceuticals at a temperature of 335 °C and at the maximum weight loss rate (350 °C).

A visual comparison of the surface of bands in the normalized FT-IR spectra indicate that the used PR, NP, and IB additives, along with their BL blend, reduce the surface of bands assigned to saturated and unsaturated hydrocarbons (CH), compounds with carbonyl groups (CO), alcohols, phenols, and esters (APE) in the composition of volatile products of the blends from the SS sample with additives. The calculated values of the ratios of band surfaces for the sample without additives (S) to the corresponding band surfaces of samples with S_{ad} additives (emitted at the temperature of 350 °C) are presented in Table 2.

The data in Table 2 clearly indicate that the greatest reduction in the surfaces of bands of hydrocarbons in the composition of volatiles is caused by the IB additive. The total surface of CH band in volatiles from the sample with IB decreases by 2.36 times, that of CO band by 2.98 times, and that of APE band by 2.51 times. The blend of pharmaceuticals containing 33.3% of the IB additive has a lower effect on reduction in CH in volatiles than the PR and NP pharmaceuticals used separately, but it is more efficient in the reduction in CO and APE than the NP additive. The presented data clearly imply that the used additives

effectively reduce the contribution of CH, CO, and APE in the composition of volatile products that can lead to the formation of PM in the products of biomass combustion [1,2].

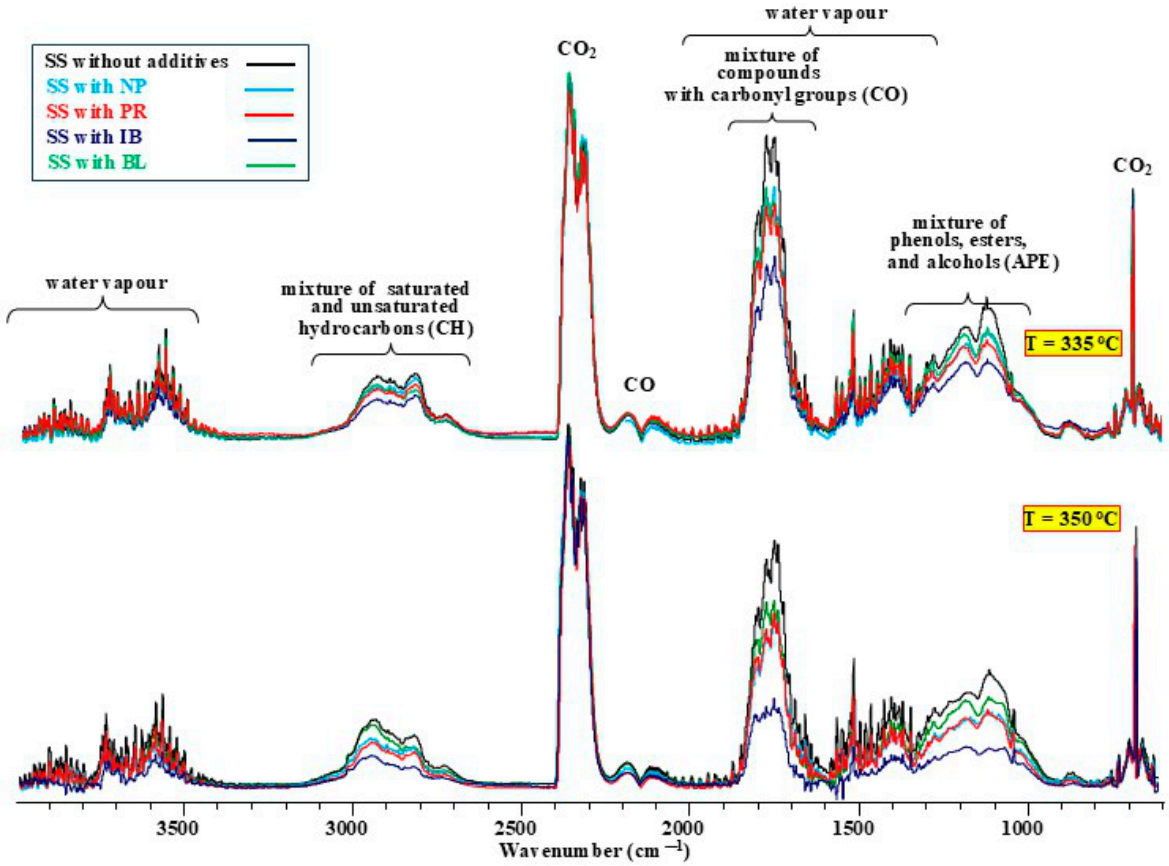

Figure 1. The FT-IR spectra of volatile products of pyrolysis from the SS sample and its blends with additives.

Table 2. The ratios of surfaces of bands in the FT-IR spectra of blends of the SS sample with additives (S_{ad}) to the corresponding bands in the FT-IR spectra of a single SS sample (S).

Sample	Band in FT-IR Spectra		
	HC (Range 3250–2500 cm^{-1})	CO (Range 1900–1600 cm^{-1})	APE (Range 1320–900 cm^{-1})
With IB	2.36 ± 0.14	2.98 ± 0.11	2.51 ± 0.15
With PR	1.33 ± 0.17	1.39 ± 0.08	1.35 ± 0.11
With NP	1.35 ± 0.12	1.23 ± 0.10	0.83 ± 0.12
With BL	1.26 ± 0.12	1.38 ± 0.15	1.17 ± 0.17

The used additives were pyrolyzed in the thermobalance in order to explain the reasons for changes that were observed in Figure 1. The TGA and DTG curves (Figure 2a,b) prove that the temperatures, at which an active decomposition of the used additives begin, vary. It should be noted that these curves are similar to those presented in the literature [34–38]. Naproxen has a softening temperature of approx. 156 °C [34], and paracetamol, 169.55 °C [35]. That is why their decomposition takes place at higher temperatures compared to ibuprofen: paracetamol intensively decomposes at T = 275 °C [35], and naproxen—at 287.0 °C [36]. The IB sample starts to decompose at a lower temperature (Figure 2a). According to Lerdkanchanaporn [37], the evaporation of ibuprofen starts at a temperature of 73.5–74.88 °C and ends when the boiling temperature is reached. Krupa et al. [38] point out that ibuprofen totally evaporates at a temperature of 250 °C. The weight loss rate of the IB additive is the highest at a temperature of

184 °C (Figure 2b). Apart from the maximum at this temperature, there are two smaller maxima near 230 and 340 °C in the DTG curve. The occurrence of these maxima influenced the shape of the TGA curve, in which some abrupt changes are present. As a result of pyrolysis, IB loses 93% of its weight. Such abrupt changes are not noticeable in the TGA curves of PR and NP samples. PR and NP completely decompose during pyrolysis whereas BL sample retains 2% of its weight after pyrolysis.

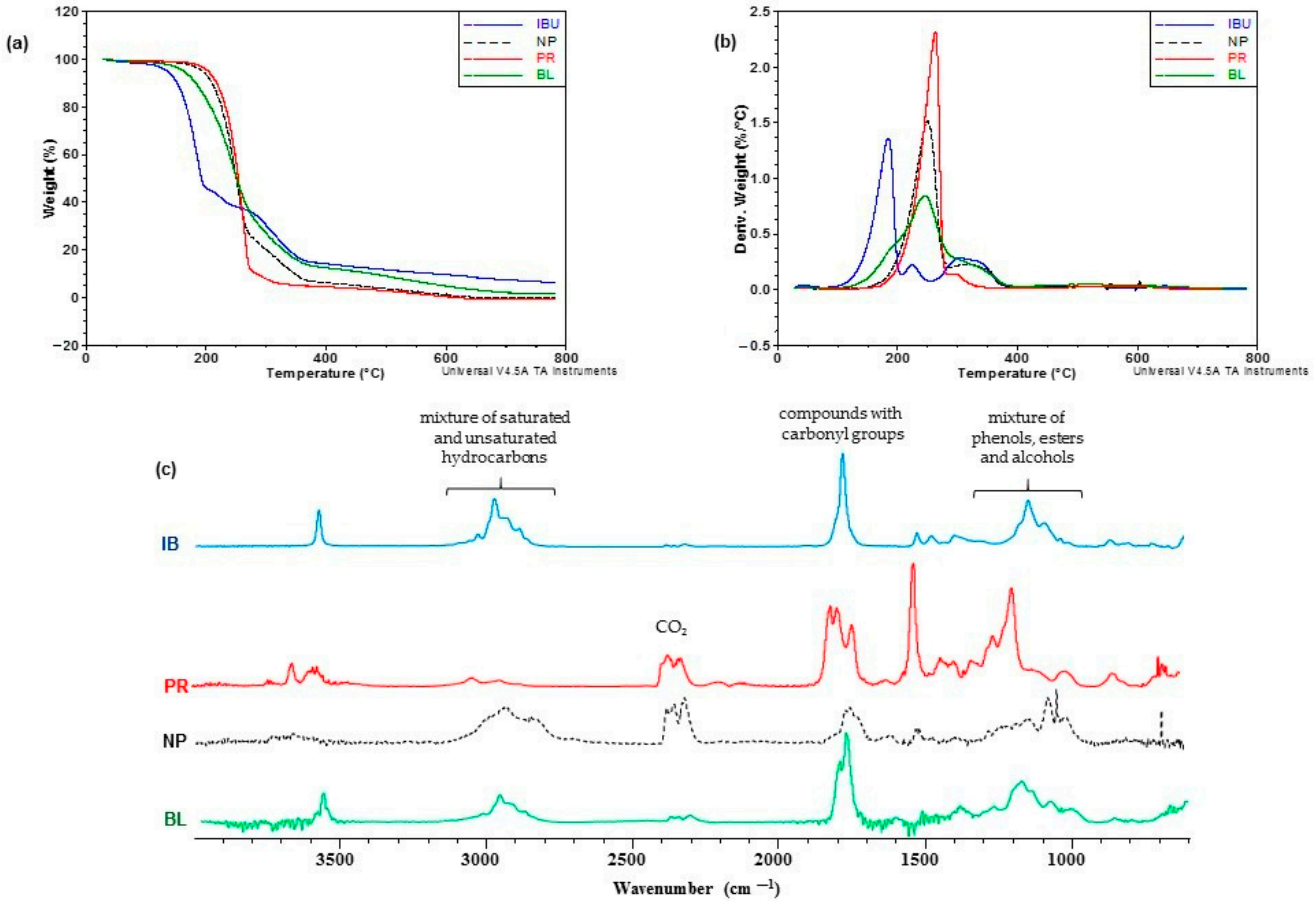

Figure 2. The TGA (**a**) and DTG (**b**) curves along the FT-IR spectra of additives (**c**).

According to the authors of works [39–41], the pyrolytic atmosphere influences the course of pyrolysis process to a great extent. The FT-IR spectra of volatiles in Figure 2c prove that the 'atmospheres' formed by the products of the decomposition of pharmaceuticals inside densified blends are different. This gives grounds to suggest that in these 'atmospheres' there are compounds that substantially differ both by the presence of functional groups and their contribution ratios. The volatile products of distinct composition as well as the radical recombination products, which were formed as a result of thermal destruction of pharmaceuticals, interact with biomass components in different ways. The IB additive has the greatest effect in reducing the contribution of hydrocarbons and compounds with carbonyl groups in the composition of volatiles (Figure 1). This additive decomposes at a temperature lower than that for other additives. That is why the products of such decomposition 'start' an active pre-treatment of SS material much earlier.

Figure S2 presents the identification data of volatile pyrolysis products of used additives based on a comparison with the Aldrich Vapor Phase Sample Library. It follows from the comparison that norcamphor is present in volatiles of IB sample, among other components (the match factor is 80.12). The software does not suggest the presence of this compound in volatile products of other pharmaceuticals. This gives rise to the assump-

tion that the presence of this compound in volatiles of IB sample can be the main reason for its greater influence on the reduction in hydrocarbons in volatile pyrolysis products. Figure 3a,b present the results of a thermogravimetric investigation of an SS sample and its blends with additives. The distinct temperatures of intensive decomposition of pharmaceuticals and the differences in composition of the products of their pyrolysis influence their interaction with SS material in various ways. The weight loss of blends with PR, NP, IB, and BL is the same at a temperature of 335 °C and totals 55.6% (Figure 3a). However, the products of decomposition of IB only cause a visible reduction in the bands of hydrocarbons in the FT-IR spectra (Figure 1).

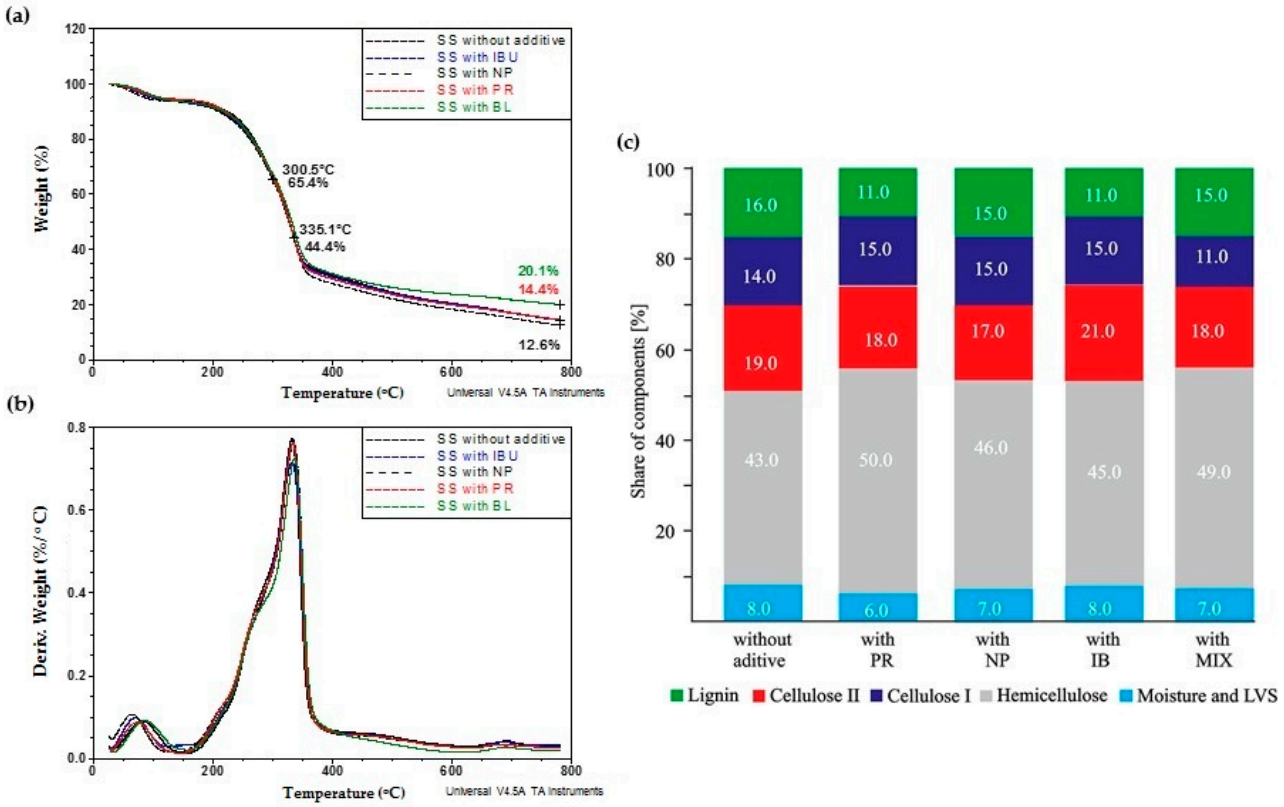

Figure 3. The TGA (**a**) and DTG (**b**) curves along with the results of the deconvolution of DTG (**c**) curves of an SS sample and its blend with additives.

The differences in shape of the TGA curves (Figure 3a) become more visible at temperatures above 350 °C. There are visible bends in the shape of the DTG curves of samples with additives in the temperature range of 270–350 °C. The occurrence of these bends implies that, under the influence of additives in this temperature range, the thermal stability of these biomass components, the weight loss of which causes the changes in shape of the DTG curves (Figure 3b), varies. The deconvolution results for these curves are presented in Figure 3c. This figure presents the values of surface areas of sub-peaks corresponding to particular biomass components. An increase in surface area of the sub-peak of the component indicates the intensification of its decomposition and a greater contribution in the formation of the DTG curve. Such an increase in surface of a peak results from a decrease in thermal stability of the component in the biomass material. The presented deconvolution results show that the contribution of hemicellulose component in the formation of the DTG curve of studied samples is much greater than that of cellulose and lignin, and changes from 43.0% to 50.4%. The values in Figure 3c are somehow higher than the values of basic biomass components determined by chemical methods as presented in the literature [42,43]. Thus, the data in Figure 3c imply that the additives change the

decomposition rate of basic biomass components in a different way. Namely, PR and IB additives restrain the decomposition of lignin, PR and NP additives do not affect the overall cellulose decomposition, whereas the BL additive inhibits it. All additives used in the investigation intensify the decomposition of hemicellulose because, under their influence, the contribution of hemicellulose in the creation of DTG curves increases. This may facilitate the reduction in hydrocarbons in volatile products. Fushimi et al. [44] also pointed out that the addition of xylan, which is a basic hemicellulose component, greatly enhances the evolution of gases (CO_2, CO, CH_4 and H_2) during its interaction with cellulose and lignin in the pyrolysis process. Moreover, while studying volatile-char interactions, Ding et al. [45] also noted that the change in composition of hemicellulose can affect these interactions and regulate the composition of volatiles. In Figure 3a,b, there are visible changes in the shape of TGA and DTG curves at temperatures above 425 °C. These changes can result from the aforementioned interactions of the chars formed from blends and the volatile products of pyrolysis, which affect the course of secondary reactions between compounds in the composition of volatiles [20,21,24,25].

3.2. Results of Spectroscopic Investigation of Studied Pyrolysis Products

The evidence of the changes in composition of the volatile products of co-pyrolysis of the studied samples is the ATR spectra of the material condensed in methanol (Figure 4).

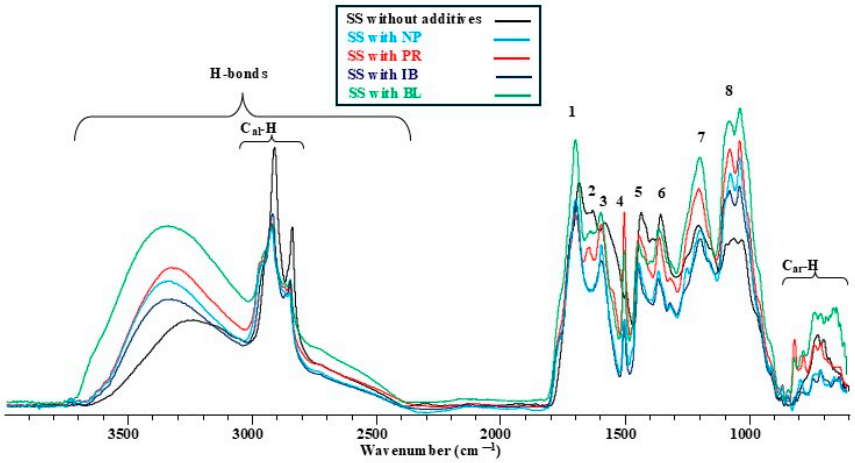

Figure 4. The normalized ATR spectra of condensates of an SS sample and its blends with additives (explanation in the text).

A comparative analysis of the normalized ATR spectra of the condensed material obtained during the co-pyrolysis of blends and single SS sample shows that the additives increase the surface area of a broad band in the range of 3700–2400 cm^{-1}. Within this range, bands from hydrogen bonds occur, indicating a greater presence of compounds with hydroxyl groups. This gives grounds to suggest that there is an increase in the amount of polar compounds capable of aggregation in the composition of studied condensates. The BL additive has a greater effect on the formation of hydrogen bonds. At the same time, the contribution of compounds of C_{al}-H type lowers in the condensates from blends with additives.

There is a reduction in height in the 1800–900 cm^{-1} wavenumber range for band 2 (quinines and quinines methides—the band of spectrum near 1657 cm^{-1}), band 5 (pyran ring symmetric scissoring C-H deformation, asymmetric in-plane fragments from lignin and hemicellulose—the band of spectrum near 1374 cm^{-1}), and band 6 (pyran ring symmetric scissoring C-H deformation, asymmetric in-plane fragments from lignin and hemicellulose—the band of spectrum near 1330 cm^{-1}). However, a height increase for bands 7 (C-O-C stretching vibration ring skeletal

pyranose—the band of spectrum near 1170 cm^{-1}) and 8 (C-O stretching in cellulose—the band of spectrum near 1080–1020 cm^{-1}) suggests that the amount of decomposition products from cellulose and lignin becomes greater in condensates. The addition of NSAIDs distinctly alters the height of bands 1 (C=O vibrations of esters, ketones, and aldehydes—the band of spectrum near 1710 cm^{-1}) and 4 (aromatic skeletal vibrations of guaiacyl rings—the band of spectrum near 1515 cm^{-1}).

Attention is drawn to the fact that the surface area of the band of C_{ar}-H vibrations in the range of 900–600 cm^{-1} increases. Such an increase indicates a rising amount of basic aromatic hydrocarbons in the condensed material. These aromatic hydrocarbons can aggregate with polar compounds and compounds capable of forming hydrogen bonds [1,2], which, in turn, reduces their release during the pyrolysis process and thus increases their presence in char. This suggestion can be confirmed by a decrease in weight loss of the SS sample with BL additive during pyrolysis at a temperature above 350 °C (Figure 3a).

Further evidence of the influence of small amounts of additives on changes in the composition of volatile pyrolysis products in the SS sample is provided by the normalized UV spectra in Figure 5. Figure 5 shows that the UV spectra of the condensates of the studied samples differ by the shape of the curves. Attention should be drawn to the spectrum of the condensate from the SS sample with NP additive which is characterized by higher values of absorbance and the presence of two distinct maxima near 205 and 225 nm. The presence of these maxima implies the presence of two groups of cyclic compounds with chromophore groups in the condensed material. In the spectrum of the condensate with BL additive near 225 nm, there is a visible maximum, but its absorbance is much lower in comparison to the absorbance of the maximum of the condensate of the SS sample with NP additive. The presence of this maximum in the curve of the condensate of the blend with BL additive can prove the influence of NP additive that is present in BL additive in the amount of 33.3%.

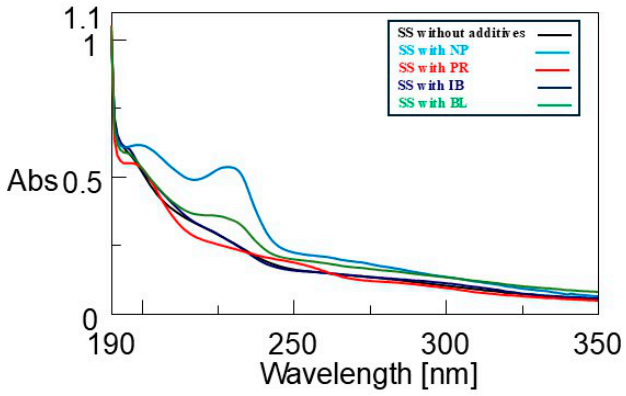

Figure 5. The normalized UV spectra of condensates of the SS sample and its blends with additives.

3.3. Results of Investigation of Chars

Figure 6a presents the diffractograms of the SS sample and its blends with additives pyrolyzed at the temperature of 450 °C, which were obtained at room temperature in the range of 2θ angles from 10 to 55 degrees. The values of the ratios of integral intensity of selected reflexes to the integral intensity of (002) reflex from NaF (parameter $A_{\gamma+char}/A_{NaF}$) were calculated.

It is noteworthy that the contribution of C atoms involved in the coherent scattering of reflected X-ray beams and in the formation of the total (002) reflex of char and the γ-fraction in the range of 15–33 degrees increased under the influence of additives. Under the influence of IB additive, this $A_{\gamma+char}/A_{NaF}$ parameter increased to the value of 1.81, and under the influence of BL additive it rose to the value of 1.96. This confirms the suggestion

about a possible increase in aggregation of basic aromatic hydrocarbons under the influence of BL additive, leading to their condensation on the surface of char.

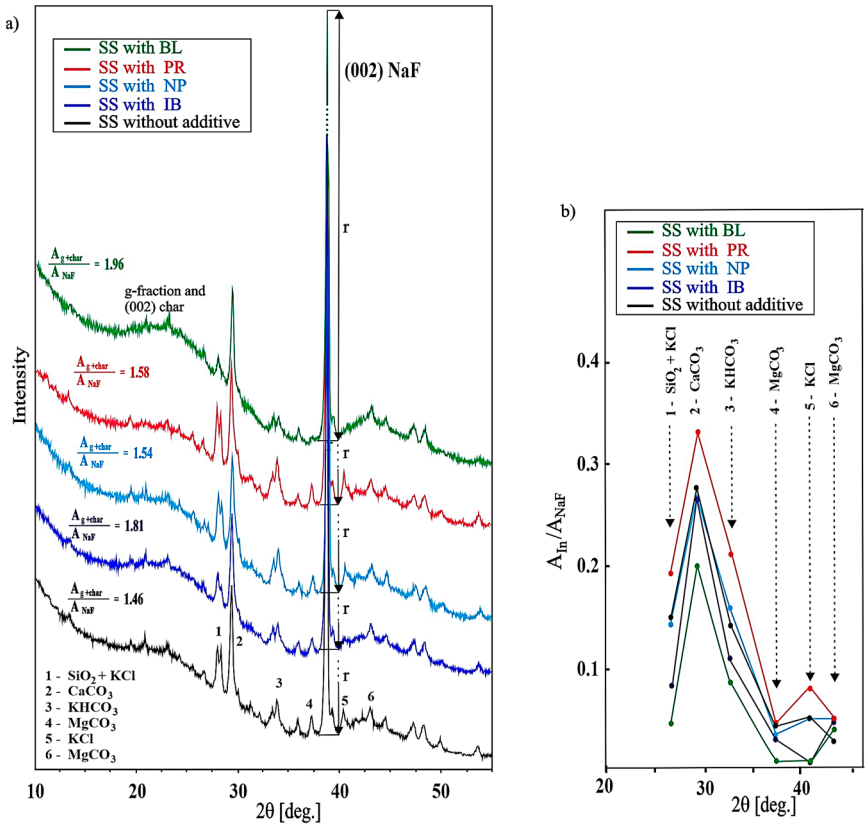

Figure 6. The diffractograms of chars from SS samples and their blends with additives (**a**) along with the results of calculation of the surface area of reflexes from inorganics to the surface area of (002) reflex from NaF (**b**).

The calculations of the surface of reflexes from inorganics imply that the ratios of their integral intensity to that of NaF (parameter A_{In}/A_{NaF} in Figure 6b) changed under the influence of used additives. The data presented in Figure 6b show that the addition of PR up to the temperature of 450 °C stops the migration of inorganics with K and Ca atoms and does not affect the migration of Mg atoms because the parameters of corresponding A_{In}/A_{NaF} are higher for the char from blend with PR additive compared to the results for the char sample without additive.

Other additives generally accelerate the release of inorganics containing K atoms from chars. At the temperature of 450 °C, the exceptions are inorganics with Mg atoms that do not migrate with volatiles, that is why their content in all chars is the same. IB and NP additives do not facilitate the release of Ca atoms up to the temperature of 450 °C, but the BL additive accelerates its migration.

The phenomenon of migration of alkali and alkaline earth metals (AAEMs) with volatile products of pyrolysis has been noticed by many researchers [27,29,40,41,46,47]. Keown et al. [28] calculated that more than 80% of inherent Na, K, Mg, and Ca atoms can be released from biomass. However, Long et al. [29] presented the following data on the release of AAEMs during the pyrolysis process: 53–76% are alkaline metals and 27–40% are alkaline earth metals. This also applies to inorganic species that can catalytically affect the thermal conversion of biomass [27,46,48]. According to Feng et al. [41], volatile AAEMs present in volatile products of biomass pyrolysis can accelerate homogeneous secondary reactions of these products. Yu et al. [49] suggest that the presence of AAEMs can change

the distribution of volatiles, increase their concentration of CO_2 and H_2, and inhibit the production of CO, CH_4, and C_2H_4. This implies that, under the influence of AAEMs present in biomass, the concentration of CO_2, H_2, and CH_4 in the composition of emitted pyrolytic gases can undergo changes [27,46,50]. Such changes are observed in Figure 1 as the change in the surface of hydrocarbon bands in the normalized FT-IR spectra of volatile pyrolysis products from the studied blends with additives.

Figure 7 presents a comparison of SEM images of similar morphological structures of piths and barks inside the chars of densified SS samples and their blends with additives that were pyrolyzed at a temperature of 750 °C. The results of quantification of peaks in the EDX spectra are placed next to the images. It is noteworthy that the amount of AAEM elements causing the appearance of peaks in the EDX spectra of chars without additives (Figure 7a,f) differs from the content of these elements in chars with additives. A comparison of the amount of K atoms in the chars of pith in Figure 7a–e implies that the addition of NP hardly changes this amount.

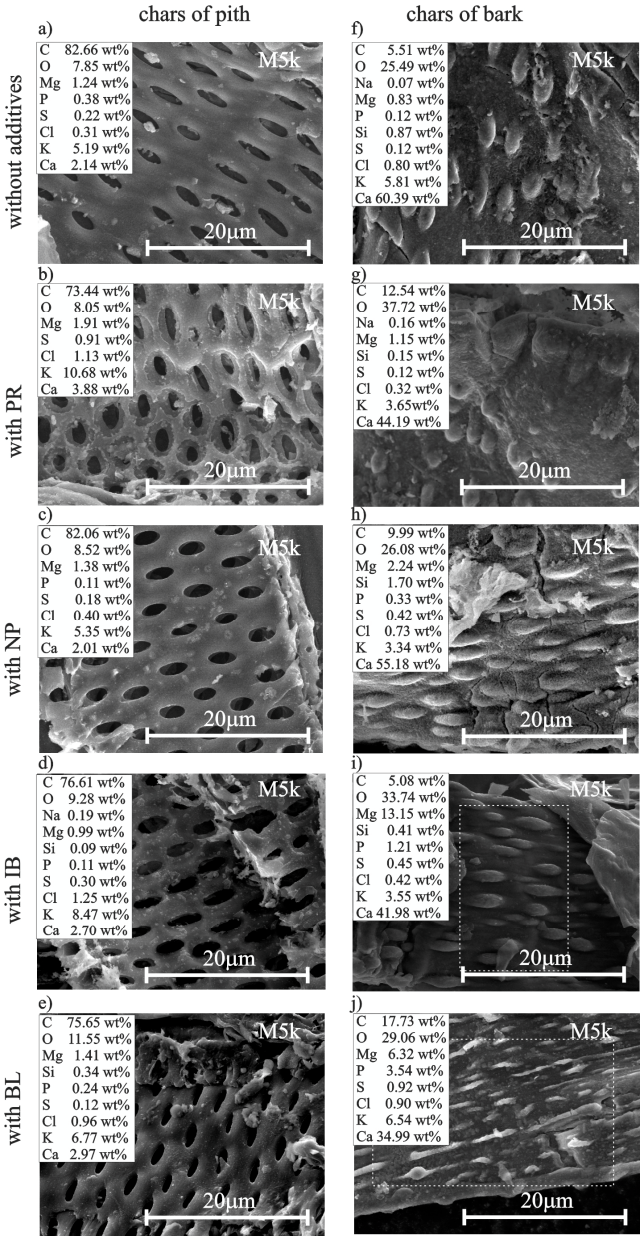

Figure 7. The SEM images of chars of pith (**a**–**e**) and chars of bark (**f**–**j**) of SS samples and their blends with additives along with the results of EDX microanalysis (explanation in the text).

The amount of K atoms in the chars of pith with BL and IB additives is somehow greater, but the PR additive inhibits the migration of this element from the appropriate char of pith. Ca and Mg atoms do not show such substantial concentration changes in their samples for chars of pith. In the morphological structures of chars of bark in the blends in Figure 7g–j, the concentration of K and Ca atoms decreases under the influence of PR, NP, and IB additives. Contrarywise, the concentration of Mg atoms increases under the influence of additives and reaches the value of 13.15 wt.% in char with IB additive (Figure 7i). The BL additive causes a smaller increase in concentration of these atoms, probably due to a lower content of IB in BL blend. The images presented in Figure 7 and the results of quantification of atoms show that different morphological structures of chars from the SS samples and their blends have distinct AAEM content and diverse ability of elements to migrate from the material of these structures together with volatile products. The IB additive had the greatest positive effect on the composition of volatile products formed during the pyrolysis of the densified sample. In char, the composition of the amount of atoms was as follows: Mg—13.15 wt.%, K—3.55 wt.%, and Ca—41.98wt.%. Zen et al. [46] observed an increase in yield of H_2 under the influence of Mg and Ca compounds. In the case of the blend with IB, a synergetic effect from inorganics that have a catalytic effect on secondary reactions in volatiles cannot be excluded.

Figure 8 presents the SEM images of morphological structures of chars of rind in the subsurface layer (Figure 8a–e) and on the surface of the chars of densified samples (Figure 8f–j). The amount of K atoms in the subsurface layer of chars with additives is greater in comparison to the amount of these atoms of chars of the sample without additives and many times higher compared to that on the surface. This gives grounds to suggest that a lower concentration of K atoms on the surface of chars is connected with an easier evaporation of these atoms from the surface of densified samples with additives but depends on the composition of volatiles that facilitate such migration. The amount of Ca atoms in the subsurface layer of chars with additives is generally higher than in chars of the sample without additives, with the exception being the sample with PR additive. The highest concentration of Ca atoms (43.27 wt.%) was determined for chars of the SS sample with IB additive, which contained Mg (7.68 wt.%), K (9.16 wt.%), and Cl (2.12 wt.%). Moreover, other atoms were also present (Figure 8i). The concentration of Mg atoms increases in the surface layer of chars of all samples, the greatest number of atoms of this element are formed in the sediment under the influence of PR additive. The chars from the subsurface and surface layers of blends with additives (apart from BL) have an increased presence of Cl atoms compared to the chars of the sample without additives, which can be a result of the influence of the addition of particular pharmaceuticals on the migration of Cl atoms with volatile products. A greater contribution of Ca, Mg, K, and Cl atoms in the char of the SS sample with IB additive implies that this set of atoms influences the reduction in hydrocarbons in volatile products of pyrolysis.

The analysis of SEM images of the subsurface and surface layers of chars in Figure 8 clearly indicates that the sediment is formed not only as a result of the loss of C atoms from the surface of chars due to their interaction with volatiles but also as a result of the condensation of material from the gas phase.

As evidenced by the shape of condensed material, the greatest amount of condensed material containing Mg atoms in the form of spheres present on the surface of char with PR additive is visible at a magnification of w M100k, as shown in Figure 9. There are two types of objects visible in the char with IB additive: spherical with dimensions from 20 to 2 μm and cubes with edge dimensions of about 10 μm. The cubes look similar to an aggregation of smaller spheres. Their composition was not determined because of the decomposition of these objects caused by a beam of electrons. It cannot be excluded that these objects may

have a catalytic effect on the composition of volatile products of pyrolysis of the SS sample with IB additive.

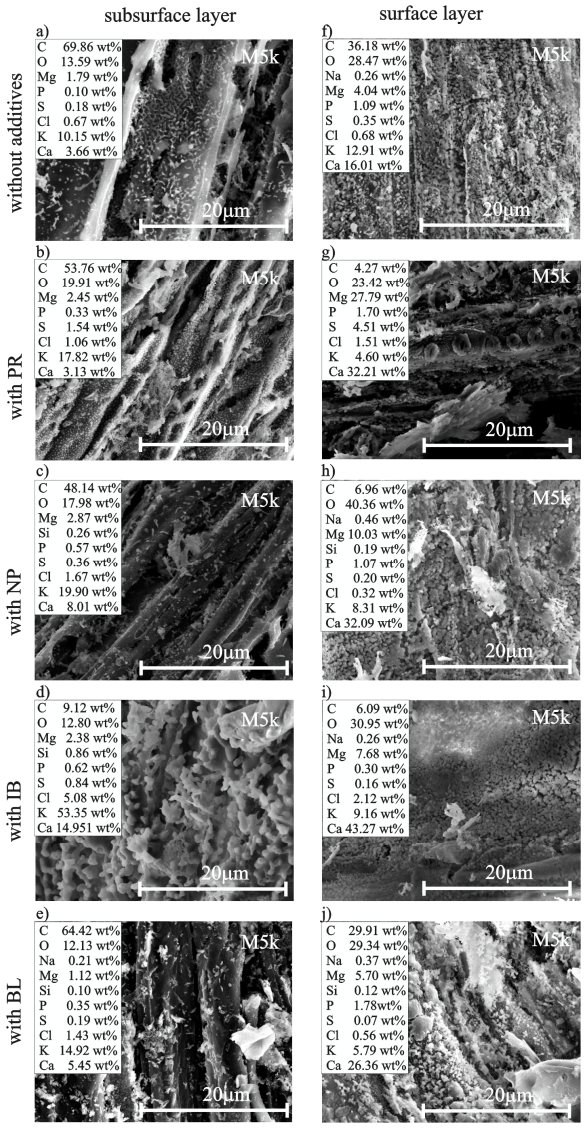

Figure 8. The SEM images of subsurface layer (**a**–**e**) and surface layer (**f**–**j**) of chars of SS sample and its blends with additives along with the results of EDX microanalysis (explanation in the text).

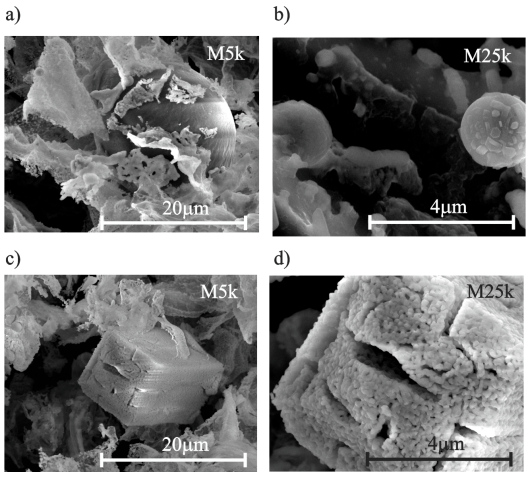

Figure 9. The SEM images of objects in chars of the SS sample with IB additive: (**a**) spherical shape at M5k, (**b**) spherical shape at M25k, (**c**) cube at M5k, and (**d**) cube at M25k.

The data above indicate clearly that the addition of expired IB, PR, NP, and BL to a SS sample affects the composition of volatile products of pyrolysis and changes the contribution of environmentally harmful hydrocarbons in them. Moreover, taking into account the measurable costs of NSAID disposal [6], expired pharmaceuticals can be disposed as a part of the energy processing of sunflower stalks, resulting in a positive effect according to the principles of circular economy.

4. Conclusions

Based on the conducted research, the following was stated:

1. The volatile products of decomposition of the used additives, such as expired paracetamol, naproxen, ibuprofen, and their blend, change the composition of volatile pyrolysis products of sunflower stalks towards reducing the contribution of saturated and unsaturated hydrocarbons, compounds with carbonyl groups, alcohols, phenols, and esters. The studied volatile decomposition products of additives reduce the contribution of undesirable hydrocarbons during energy recovery from sunflower stalks.
2. Among the studied NSAIDs, ibuprofen was the most effective. At a temperature of 350 °C, there was a reduction in the amount of saturated and unsaturated hydrocarbons in volatiles by about 2.36 times, by 2.5 times for alcohols, phenols, and esters, and by 3 times for compounds with carbonyl groups.
3. The obtained results give grounds to suggest that the primary reason for the effectiveness of ibuprofen in the reduction in hydrocarbons in the composition of volatiles is its low temperature of thermal decomposition. The formed products of evaporation of ibuprofen make a pre-treatment of biomass material, accelerating the decomposition of cellulose and hemicellulose.
4. During pyrolysis of expired pharmaceuticals without additives and their blend, a diverse atmosphere of compounds with distinct functional groups is formed. The second reason for the distinct influence of the additives on the thermal stability of components in the material of the SS sample is the differences in composition of the products of decomposition of expired pharmaceuticals.
5. All additives facilitate an increase in the contribution of compounds capable of forming hydrogen bonds in the composition of condensed volatile material. This promotes their aggregation and greater ordering of C atoms inside the chars of samples with additives at a temperature of 450 °C. These processes occur in the char with BL additive to a greater extent, which results in a decrease in its weight loss.
6. The used additives influence the changes in the migration rate of inherent AAEMs during pyrolysis of the SS sample. The addition of paracetamol inhibits the migration of AAEMs up to a temperature of 450 °C. On the surface of chars with additives, a sediment is formed that has a greater contribution of Ca and Mg atoms than in the char without additives. Such composition of sediment can favor the reduction in hydrocarbons during the interaction between volatiles and char.
7. The volatile AAEMs present in the gas phase of volatile products of pyrolysis initiate secondary reactions between volatile products of biomass pyrolysis, are condensed on the surface of chars, and actively participate in intensification of the interaction between volatiles and chars. Under the influence of naproxen, cyclic compounds with chromophore groups are formed in volatile products, whereas under the influence of ibuprofen, the volatile products of biomass pyrolysis are condensed and form aggregates of various geometric shape and size.
8. Thus, the conducted research proved that the process of energy recovery from the agricultural waste of sunflower stalks can be optimized with small amounts (about 2

wt.%) of expired pharmaceuticals according to the principles of circular economy in a way that reduces pollution of the environment with harmful substances.

Supplementary Materials: The following supporting information can be downloaded at: https://www.mdpi.com/article/10.3390/en18061509/s1, Figure S1: Results of fitting of curves DTG; Figure S2: The identification data of volatile pyrolysis products of used additives based on a comparison with the Aldrich Vapor Phase Sample Library.

Author Contributions: Conceptualization, A.S. and V.Z.; methodology, A.S. and V.Z.; software, A.S. and V.Z.; validation, A.S. and V.Z.; investigation, A.S., V.Z. and S.B.; resources, A.S.; data curation, A.S. and V.Z.; writing—original draft preparation, A.S. and V.Z.; writing—review and editing, A.S. and V.Z.; visualization, A.S.; supervision, V.Z.; project administration, A.S.; funding acquisition, V.Z. All authors have read and agreed to the published version of the manuscript.

Funding: This research was funded by Jan Kochanowski University in Kielce, grant number SUPB.RN. 24.216.

Data Availability Statement: The data presented in this study are available on request from the corresponding author.

Acknowledgments: The authors thank A. Gałuszka and J. Masternak V. for their help in obtaining the results of ultimate analysis and the analysis of the composition of inorganics. This research was supported in part by the Excellence Initiative—Research University Program at the Jagiellonian University in Kraków.

Conflicts of Interest: The authors declare no conflicts of interest.

Abbreviations

The following abbreviations are used in this manuscript:

AAEMs	alkali and alkaline earth metals
PM	particulate matters
SS	sunflower stalks
NP	naproxen
PR	paracetamol
IB	ibuprofen
BL	blend
HHV	higher heating value
NSAIDs	non-steroidal anti-inflammatory drugs

References

1. Samae, H.; Tekasakul, S.; Tekasakul, P.; Furuuchi, M. Emission factors of ultrafine particulate matter (PM < 0.1 μm) and particle-bound polycyclic aromatic hydrocarbons from biomass combustion for source apportionment. *Chemosphere* **2021**, *262*, 127846. [CrossRef] [PubMed]
2. Sun, J.; Shen, Z.; Zhang, Y.; Zhang, Q.; Wang, F.; Wang, T.; Chang, X.; Lei, Y.; Xu, H.; Cao, J.; et al. Effects of biomass briquetting and carbonization on PM2.5 emission from residential burning in Guanzhong Plain, China. *Fuel* **2019**, *244*, 379–387. [CrossRef]
3. Mgharbel, M.; Halawy, L.; Milane, A.; Zeaiter, J.; Saad, W. Pyrolysis of pharmaceuticals as a novel means of disposal and material recovery from waste for a circular economy. *J. Anal. Appl. Pyrol.* **2023**, *172*, 106014. [CrossRef]
4. Zubkova, V.; Strojwas, A.; Kaniewski, M.; Jany, B.R. The influence of the additives of expired paracetamol (PR) and naproxen (NP) on the thermal behaviour of high volatile bituminous coal (HVBC) and the composition of material extracted from the zones of its plastic layer. *Fuel* **2020**, *273*, 117752. [CrossRef]
5. Zubkova, V.; Strojwas, A.; Kaniewski, M.; Ziomber, S. Investigation of influence of the additives of expired paracetamol (PR) and naproxen (NP) on the changes in volume of heated charge of a higher rank coal. *Fuel* **2018**, *217*, 605–616. [CrossRef]
6. Strojwas, A.; Zubkova, V.; Banas, D.; Stabrawa, I. The Influence of Addition of Expired Pharmaceuticals on Thermal Behaviour of Selected Types of Biomass. *Energies* **2024**, *17*, 2809. [CrossRef]

7. Yang, H.; Yan, R.; Chen, H.; Lee, D.H.; Zheng, C. Characteristics of hemicellulose, cellulose and lignin pyrolysis. *Fuel* **2007**, *86*, 1781–1788. [CrossRef]
8. Usino, D.O.; Supriyanto; Ylitervo, P.; Pettersson, A.; Richards, T. Influence of temperature and time on initial pyrolysis of cellulose and xylan. *J. Anal. Appl. Pyrol.* **2020**, *147*, 104782. [CrossRef]
9. Yang, H.; Li, S.; Liu, B.; Chen, Y.; Xiao, J.; Dong, Z.; Gong, M.; Chen, H. Hemicellulose pyrolysis mechanism based on functional group evolutions by two-dimensional perturbation correlation infrared spectroscopy. *Fuel* **2020**, *267*, 117302. [CrossRef]
10. Chen, H.; Che, Q.; Li, S.; Liu, Z.; Yang, H.; Chen, Y.; Wang, X.; Shao, J.; Chen, H. Recent developments in lignocellulosic biomass catalytic fast pyrolysis: Strategies for the optimization of bio-oil quality and yield. *Fuel Process. Technol.* **2019**, *196*, 106180. [CrossRef]
11. Worasuwannarak, N.; Sonobe, T.; Tanthapanichakoon, W. Pyrolysis behaviors of rice straw, rice husk, and corncob by TG-MS technique. *J. Anal. Appl. Pyrol.* **2007**, *78*, 265–271. [CrossRef]
12. Zhang, J.; Choi, Y.S.; Yoo, C.G.; Kim, T.H.; Brown, R.C.; Shanks, B.H. Cellulose-hemicellulose, cellulose-lignin interactions during fast pyrolysis. *ACS Sustain. Chem. Eng.* **2015**, *3*, 293–301. [CrossRef]
13. Liu, Q.; Zhong, Z.; Wang, S.; Luo, Z. Interactions of biomass components during pyrolysis: A TG-FTIR study. *J. Anal. Appl. Pyrol.* **2011**, *90*, 213–218. [CrossRef]
14. Bielecki, M.; Zubkova, V. Analysis of Interactions Occurring during the Pyrolysis of Lignocellulosic Biomass. *Molecules* **2023**, *28*, 506. [CrossRef]
15. Ajorloo, M.; Ghodrat, M.; Scott, J.; Strezov, V. Evaluating the role of feedstock composition and component interactions on biomass gasification. *Fuel* **2025**, *381*, 133528. [CrossRef]
16. Nocquet, T.; Dupont, C.; Commandre, J.-M.; Grateau, M.; Thiery, S.; Salvador, S. Volatile species release during torrefaction of wood and its macromolecular constituents: Part 1—Experimental study. *Energy* **2014**, *72*, 180–187. [CrossRef]
17. Chen, Y.; Fang, Y.; Yang, H.; Xin, S.; Zhang, X.; Wang, X.; Chen, H. Effect of volatiles interaction during pyrolysis of cellulose, hemicellulose, and lignin at different temperatures. *Fuel* **2019**, *248*, 1–7. [CrossRef]
18. Hosoya, T.; Kawamoto, H.; Saka, S. Solid/liquid- and vapor-phase interactions between cellulose- and lignin-derived pyrolysis products. *J. Anal. Appl. Pyrol.* **2009**, *85*, 237–246. [CrossRef]
19. Yang, H.; Liu, M.; Chen, Y.; Xin, S.; Zhang, X.; Wang, X.; Chen, H. Vapor–solid interaction among cellulose, hemicellulose and lignin. *Fuel* **2020**, *263*, 116681. [CrossRef]
20. Giudicianni, P.; Cardone, G.; Sorrentino, G.; Ragucci, R. Hemicellulose, cellulose and lignin interactions on Arundo donax steam assisted pyrolysis. *J. Anal. Appl. Pyrol.* **2014**, *110*, 138–146. [CrossRef]
21. Eom, I.Y.; Kim, J.Y.; Kim, T.S.; Lee, S.M.; Choi, D.; Choi, I.G.; Choi, J.W. Effect of essential inorganic metals on primary thermal degradation of lignocellulosic biomass. *Bioresour. Technol.* **2012**, *104*, 687–694. [CrossRef]
22. Zhang, L.; Duan, F.; Huang, Y. Thermogravimetric investigation on characteristic of biomass combustion under the effect of organic calcium compounds. *Bioresour. Technol.* **2015**, *175*, 174–181. [CrossRef] [PubMed]
23. Collard, F.-X.; Blin, J.; Bensakhria, A.; Valette, J. Influence of impregnated metal on the pyrolysis conversion of biomass constituents. *J. Anal. Appl. Pyrol.* **2012**, *95*, 213–226. [CrossRef]
24. Hu, S.; Jiang, L.; Wang, Y.; Su, S.; Sun, L.; Xu, B.; He, L.; Xiang, J. Effects of inherent alkali and alkaline earth metallic species on biomass pyrolysis at different temperatures. *Bioresour. Technol.* **2015**, *192*, 23–30. [CrossRef]
25. Xia, S.; Li, K.; Xiao, H.; Cai, N.; Dong, Z.; Chen, X.; Chen, Y.; Yang, H.; Tu, X.; Chen, H. Pyrolysis of Chinese chestnut shells: Effects of temperature and Fe presence on product composition. *Bioresour. Technol.* **2019**, *287*, 121444. [CrossRef]
26. Guo, F.; Liu, Y.; Wang, Y.; Li, X.; Li, T.; Guo, C. Pyrolysis kinetics and behavior of potassium-impregnated pine wood in TGA and a fixed-bed reactor. *Energy Convers. Manag.* **2016**, *130*, 184–191. [CrossRef]
27. Chen, X.; Chen, Y.; Yang, H.; Chen, W.; Wang, X.; Chen, H. Fast pyrolysis of cotton stalk biomass using calcium oxide. *Bioresour. Technol.* **2017**, *233*, 15–20. [CrossRef]
28. Keown, D.M.; Favas, G.; Hayashi, J.-I.; Li, C.-Z. Volatilisation of alkali and alkaline earth metallic species during the pyrolysis of biomass: Differences between sugar cane bagasse and cane trash. *Bioresour. Technol.* **2005**, *96*, 1570–1577. [CrossRef]
29. Long, J.; Song, H.; Jun, X.; Sheng, S.; Sun, L.-S.; Xu, K.; Yao, Y. Release characteristics of alkali and alkaline earth metallic species during biomass pyrolysis and steam gasification process. *Bioresour. Technol.* **2012**, *116*, 278–284. [CrossRef]
30. Meng, F.; Wang, D. Effects of vacuum freeze drying pretreatment on biomass and biochar properties. *Renew. Energ.* **2020**, *155*, 1–9. [CrossRef]
31. Jia, D.; Liang, J.; Liu, J.; Chen, D.; Evrendilek, F.; Wen, T.; Cao, H.; Zhong, S.; Yang, Z.; He, Y. Insights into pyrolysis of ginger via TG-FTIR and Py-GC/MS analyses: Thermochemical behaviors, kinetics, evolved gas, and products. *J. Anal. Appl. Pyrol.* **2024**, *179*, 106442. [CrossRef]
32. Zubkova, V.; Strojwas, A.; Bielecki, M.; Kieush, L.; Koverya, A. Comparative study of pyrolytic behavior of the biomass wastes originating in the Ukraine and potential application of such biomass. Part 1. Analysis of the course of pyrolysis process and the composition of formed products. *Fuel* **2019**, *254*, 115688. [CrossRef]

33. Janković, B.; Manić, N.; Stojiljković, D.; Jovanović, V. TSA-MS characterization and kinetic study of the pyrolysis process of various types of biomass based on the Gaussian multi-peak fitting and peak-to-peak approaches. *Fuel* **2018**, *234*, 447–463. [CrossRef]
34. Ramos, P.; Raczak, B.K.; Silvestri, D.; Wacławek, S. Application of TGA/c-DTA forDistinguishing between Two Forms of Naproxen in PharmaceuticalPreparations. *Pharmaceutics* **2023**, *15*, 1689. [CrossRef] [PubMed]
35. Oliveira, G.G.G.; Feitosa, A.; Loureiro, K.; Fernandes, A.R.; Souto, E.B.; Severino, P. Compatibility study of paracetamol, chlorpheniramine maleate and phenylephrine hydrochloride in physical mixtures. *Saudi Pharm. J.* **2017**, *25*, 99–103. [CrossRef]
36. Sovizi, R.M. Thermal behavior of drugsInvestigation on decomposition kinetic of naproxen and celecoxib. *J. Therm. Anal. Calorim.* **2010**, *102*, 285–289. [CrossRef]
37. Lerdkanchanaporn, S. A thermal analysis study of ibuprofen and starch mixtures using simultaneous TG-DTA. *Thermochim. Acta* **1999**, *340–341*, 131–138. [CrossRef]
38. Krupa, A.; Majda, D.; Jachowicz, R.; Mozgawa, W. Solid-state interaction of ibuprofen and Neusilin US2. *Thermochim. Acta* **2010**, *509*, 12–17. [CrossRef]
39. Li, C.; Zhang, C.; Sun, K.; Zhang, Z.; Zhang, L.; Zhang, S.; Liu, Q.; Hu, G.; Wang, S.; Hu, X. Pyrolysis of saw dust with co-feeding of methanol. *Renew. Energy* **2020**, *160*, 1023–1035. [CrossRef]
40. Zhang, Z.; Liu, J.; Shen, F.; Wang, Z. Temporal release behavior of potassium during pyrolysis and gasification of sawdust particles. *Renew. Energy* **2020**, *156*, 98–106. [CrossRef]
41. Feng, D.; Shang, Q.; Song, Y.; Wang, Y.; Cheng, Z.; Zhao, Y.; Sun, S. In-situ catalytic synergistic interaction between self-contained K and added Ni in biomass fast/slow pyrolysis. *Renew. Energy* **2024**, *222*, 119889. [CrossRef]
42. Ristanović, V.; Primorac, D.; Dorić, B. The Importance of Green Investments in Developed Economies—MCDM Models for Achieving Adequate Green Investments. *Sustanaibility* **2023**, *15*, 6341. [CrossRef]
43. Vital Brazil, O.A.; Vilanova-Neta, J.L.; Oliveira Silva, N.; Monteiro Vieira, I.M.; Silva Lima, A.; Santos Ruzene, D.; Pereira Silva, D.; Figueiredo, R.T. Integral use of lignocellulosic residues from different sunflower accessions: Analysis of the production potential for biofuels. *J. Clean. Prod.* **2019**, *221*, 430–438. [CrossRef]
44. Fushimi, C.; Katayama, S.; Tsutsumi, A. Elucidation of interaction among cellulose, lignin and xylan during tar and gas evolution in steam gasification. *J. Anal. Appl. Pyrol.* **2009**, *86*, 82–89. [CrossRef]
45. Ding, K.; Wang, Y.; Liu, S.; Lin, G.; Syed-Hassan, S.S.A.; Li, B.; Hu, X.; Huang, Y.; Zhang, S.; Zhang, H. Volatile-char interactions during biomass pyrolysis: Insight into the activity of chars derived from three major components. *J. Anal. Appl. Pyrol.* **2021**, *159*, 105320. [CrossRef]
46. Zeng, K.; Yang, Q.; Zhang, Y.; Mei, Y.; Wang, X.; Yang, H.; Shao, J.; Li, J.; Chen, H. Influence of torrefaction with Mg-based additives on the pyrolysis of cotton stalk. *Bioresour. Technol.* **2018**, *261*, 62–69. [CrossRef]
47. Chen, X.; Li, S.; Liu, Z.; Chen, Y.; Yang, H.; Wang, X.; Che, Q.; Chen, W.; Chen, H. Pyrolysis characteristics of lignocellulosic biomass components in the presence of CaO. *Bioresour. Technol.* **2019**, *287*, 121493. [CrossRef]
48. Tian, X.; Wang, Y.; Zeng, Z.; Dai, L.; Peng, Y.; Jiang, L.; Yang, X.; Yue, L.; Liu, Y.; Ruan, R. Study on the mechanism of co-catalyzed pyrolysis of biomass by potassium and calcium. *Bioresour. Technol.* **2021**, *320*, 124415. [CrossRef]
49. Yu, J.; Guo, Q.; Gong, Y.; Ding, L.; Wang, J.; Yu, G. A review of the effects of alkali and alkaline earth metal species on biomass gasification. *Fuel Process. Technol.* **2021**, *214*, 106723. [CrossRef]
50. Yang, H.; Wang, D.; Li, B.; Zeng, Z.; Qu, L.; Zhang, W.; Chen, H. Effects of potassium salts loading on calcium oxide on the hydrogen production from pyrolysis-gasification of biomass. *Bioresour. Technol.* **2018**, *249*, 744–750. [CrossRef]